Equilibrium phase transitions in a porous medium

T. MacFarland* and G. T. Barkema†
Laboratory of Atomic and Solid State Physics,
Clark Hall, Cornell University, Ithaca, New York 14853-2501

J. F. Marko
Center for Studies in Physics and Biology,
The Rockefeller University, 1230 York Avenue, New York, New York 10021-6399
(Received 22 June 1995)

Static critical phenomena of a three-dimensional Ising model confined in a porous medium made by spinodal decomposition have been studied using large-scale Monte Carlo simulations. We thus examine the influence of the geometry of Vycor-like materials on phase transitions. No surface interactions (preference of the Vycor-like material for one phase above the other) are taken into account. We find that the critical temperature depends on the average pore size D as $T_c(D)=T_c(\infty)-c/D$. The critical exponents are independent of pore size: we find $\nu=0.8\pm0.1$, $\gamma=1.4\pm0.1$, $\beta=0.65\pm0.13$. No divergence is observed for the specific heat, indicating $\alpha\leqslant 0$. All data for all pore sizes can be collapsed well with the scaling function for the magnetic susceptibility $\chi L^{-\gamma/\nu}=\tilde{\chi}(tL^{1/\nu})$, where $t=T/T_c(D)-1$. These critical phenomena are consistent with those computed for the randomly site-diluted Ising model. Experimental realizations of our numerical experiments are discussed.

I. INTRODUCTION

Fluids confined to porous media are of basic experimental and theoretical interest. Recent reports on the critical point of the liquid-vapor coexistence lines of ^{4}He (Ref. 1) and N_2 (Ref. 2) in aerogel, as well as on the phase separation of liquid mixtures in Vycor[3–5] and of ^{3}He-^{4}He mixtures[6] in aerogel, suggests that the critical behavior of these systems may be profoundly modified. Some experiments suggest that while the coexistence regions are narrowed over a range of temperatures below T_c, the universality class of the transitions remains the same as in the bulk homogeneous systems. There is also some experimental evidence[3–5,7] for different critical exponents for phase-separation and liquid-vapor transitions in Vycor, aerogel, and other porous media. Questions of exponents are thus far from settled.

Various theoretical directions have recently been taken in order to try to understand phase transitions in porous media. When the pore surfaces couple differently to the two components of a phase-separating mixture, it has been argued that one might expect random-field Ising critical phenomena.[8] In the case where a ^{3}He-^{4}He mixture is confined to the interior of an aerogel, recent theories and calculations[9,10] indicate that the λ point (the low-temperature terminus of the second-order superfluid transition line) is moved to zero temperature, causing phase separation to occur inside the superfluid phase. Mounting theoretical evidence indicates that symmetry-breaking phase transitions may be changed from first to second order by the presence of aerogel-like media.[9,11]

In this work, we find that the exclusion of a two-component liquid from the glassy region of a porous medium can modify its static critical exponents. We do not include symmetry-breaking interactions between the porous medium and the mixture inside it. We have chosen to focus on Vycor-like media made via spinodal decomposition,[12,13] rather than on aerogels, which are made by poorly understood aggregation processes. Using a recently developed algorithm[14] we are able to efficiently simulate spinodal decomposition, and so to construct porous media that should have a geometry very similar to that of Vycor glass. This first step is described in Sec. II.

Once we have our model Vycor, we can study phase transitions in a mixture introduced into its pores. Because the liquid phase transitions that are the subject of our interest in this work are in the same universality class as the Ising ferromagnet, the natural model for a liquid mixture put into the Vycor pores is the Ising model. The extraction of equilibrium properties from the resulting ''Ising model on a porous lattice'' is an arduous computational task. Therefore a parallel Monte Carlo (MC) cluster algorithm developed for the simulation of Ising systems on parallel computers,[15] together with the Wolff[16] cluster algorithm have been used, on a $KSR-1$ parallel supercomputer. This is described in Sec. V.

In Sec. VI our results are discussed. We find that our Ising model in model Vycor has a critical phase transition at a temperature shifted down from that of the pure Ising model by an amount $\propto 1/D$, where D is the pore diameter. Over a range of pore sizes we find the same critical exponents; in fact, magnetic susceptibility data for all pore sizes may be described by one scaling function. The exponents are consistent with those of the randomly diluted Ising model (also called the random Ising model, or the random-temperature Ising model). We argue that this identification is reasonable since the broken bonds at pore surfaces (essentially the perturbation to the pure Ising Hamiltonian) have uncorrelated statistics at long distances, and do not break spin-reversal symmetry.

II. MODELING VYCOR WITH PHASE SEPARATION IN AN ISING MODEL

Vycor is made by mixing two types of glass, letting them phase separate for a short time, halting the phase separation

by cooling, and finally etching away one of the two types of glass.[12] The simplest models for this phase-separation process are dynamical Ising models with locally conserved magnetization.[13] In this section we describe the simulation of the production of Vycor, using phase separation in a three-dimensional Ising model.

A. Method

In earlier work[14] we studied properties of domain growth via spinodal decomposition in the three-dimensional (3D) Ising model. The Hamiltonian of the Ising model that is used to generate the porous medium configuration is

$$H_{\mathrm{PM}}/k_B T = -J_{\mathrm{PM}} \sum_{\langle i,j \rangle} \sigma_i \sigma_j , \tag{1}$$

where $\langle i,j \rangle$ denotes a pair of neighboring sites, and J_{PM} is the dimensionless coupling. The spins σ_i are located at positions r_i on a simple-cubic lattice with periodic boundary conditions and edge length L. Each spin can take the values ± 1, representing the two types of glass. For this work, all coarsening took place at $J = 1.67 J_c$, where $J_c \approx 0.22$ is the critical coupling of the pure Ising model on a cubic lattice.

In a simulation of the production process of Vycor, one starts with a three-dimensional lattice on which a spin is located at each site, randomly pointing upwards or downwards, modeling the mixture of the two types of glass. Next, this Ising model configuration is simulated over a finite time at a temperature $J_{\mathrm{PM}} = 1.67 J_c$, using spin-exchange MC kinetics, which causes the $+$ and $-$ spins to separate into domains. We have used an algorithm that was developed specifically for this purpose and is described elsewhere.[14]

After some time, this phase-separation process is halted, and the upwards-pointing spins are removed, to model the quenching of the domain structure followed by the etching away of one type of glass. The downward-pointing spins constitute our model of the remaining Vycor glass. Finally, small cavities that are inaccessible from the outside are filled since the binary mixture to be studied in the Vycor will be introduced from the outside and will be unable to get to such isolated holes. For the configurations we studied, the volume fraction of these removed cavities is tiny: in the runs described below, such cavities comprise less than 0.2% of the total volume.

B. Properties of model Vycor

The ''void'' and ''glass'' regions resulting from the process described above are statistically identical because of up-down symmetry during the growth process. The porous medium consists of one large ''glass'' region permeated by one large pore. In Fig. 1 we show three typical examples of model structures of porous media that we obtained in this way for systems of 64^3 lattice sites.

Of importance in our characterization of the porous media, insofar as the properties and critical behavior of a liquid confined to such a medium are concerned, is what we refer to as the medium's pore size. This may be extracted from the structure factor $S(k)$ of our porous media:

$$S(k) = \left| \sum_j e^{i\mathbf{k}\cdot\mathbf{r}_j} \sigma_j \right|^2 . \tag{2}$$

During spinodal decomposition, the structure factor $S(k)$ of the spins converges towards a shape independent of the length of the annealing time and temperature. The main feature of $S(k)$ is a peak at some k^*. At low k, $S(k)$ increases as a power law which is theoretically predicted to be k^4 (Ref. 17) (although recent work suggests that this exponent might be smaller[14]); at large k, $S(k)$ decreases as k^{-4}, a behavior known as Porod's law.[13] The sharpness of the peak tells us that the pores in a porous medium have a well-defined typical size $D \sim 1/k^*$. This D grows in time during the phase-separation process as $D \sim t^{1/3}$, in agreement with theoretical arguments of Lifshitz, Slyozov, and Wagner.[18]

To be more definite, we take the pore size

$$D = \pi / \langle k \rangle , \tag{3}$$

where $\langle k \rangle$ is the first moment of $S(k)$:

$$\langle k \rangle = \frac{\int_0^\infty k S(k) dk}{\int_0^\infty S(k) dk} . \tag{4}$$

This definition of the pore size is often used to measure the domain size during spinodal decomposition simulations.[19] A visual inspection of our Vycor configurations shows that D is a good measure of the typical pore size of these systems. The three structures in Fig. 1 have average pore sizes of $D = 1.6$, 2.2, and 7.9.

Figure 2 shows a plot of the pore size D as a function of growth time, together with the $t^{1/3}$ asymptote. We label the points that correspond to configurations used in this work. The pore sizes of those configurations are given in the second column of Table I, and we present the scaled structure factors of the spin density of those porous medium configurations in Fig. 3. The configurations with small pore sizes are still far from the regime where the structure function collapses, but for this work that is not essential.

The fact that $S(k)$ approaches zero according to a power law for small k indicates that the mass density is correlated over long ranges. It is not the spin density, however, that is most relevant to our study of mixtures confined in a porous medium, but rather the density of the surface area of the pores and the range of pore correlations. This is simply because the ''broken bonds'' in the Ising model to be put into the voids of our model Vycor are on the pore surfaces.

We have computed the pore surface areal density and its structure factor, averaged over seven realizations at each pore size. The results are shown in Fig. 4, which shows that in each case, in contrast with the structure factor of the porous medium density, the areal structure factor approaches a constant for small wave vectors. This is to be expected since the spin-exchange dynamics certainly do not conserve total interface area during phase separation. So, even though the pore volume distribution is correlated at long ranges, the pore surface distribution is not. The consequences of this for the critical phenomena will be discussed in the next section.

III. MODELING THE BINARY MIXTURE INSIDE VYCOR

We want to examine the static critical phenomena of a binary liquid inside the pores defined by the phase-separation process described in the previous section. The Ising model describes both liquid-vapor criticality, and critical demixing

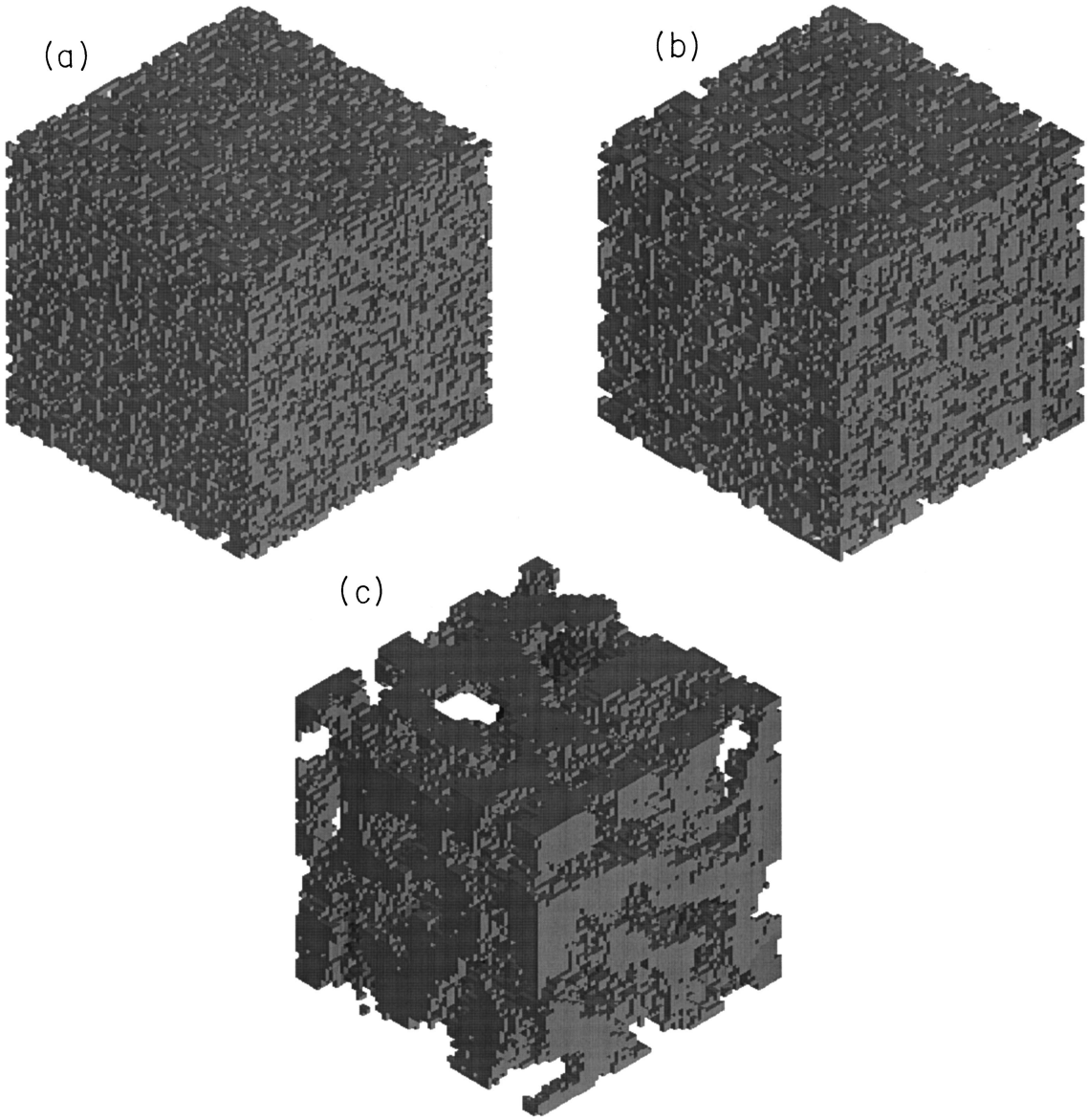

FIG. 1. Three typical examples of the model porous medium structures to which we confined the Ising model. The samples are quenched at $t=0$ from a high temperature to $T=0.6T_c$, and coarse grained for $t=10$ (a), $t=100$ (b), and $t=10\,000$ time steps (c). The pore sizes for these samples are $D=1.41$, $D=2.24$, and $D=7.92$, resp.

of binary liquids. So, the Ising model inside our model pores is a reasonable starting point for describing the critical behavior of either of those systems confined inside Vycor.

In the porous medium configurations generated previously, we defined a ''glass'' region from which the liquid is supposed to be excluded. The remaining empty ''pore'' region provides the lattice upon which the spin variables of a second Ising system are defined. The equilibrium properties of this Ising system are defined by the Hamiltonian

$$H/k_BT=-J\sum_{\langle i,j\rangle}\sigma_i\sigma_j, \tag{5}$$

where the summation runs over all pairs of neighboring sites in the ''pore'' region. We will use the dimensionless coupling J and the dimensionless temperature $T\equiv 1/J$ to describe our results.

In this paper we have not studied interactions between the mixture and the pore surfaces; understanding (5) is already a challenging problem. In most experiments we expect the pore surfaces to have different contact energies with each component, which in our model would break the spin-reversal symmetry of (5). The simplest such interactions would be surface ''fields'' that would favor one spin over the other at the pore surfaces. The absence of such interactions in (5) prevents us from making a direct comparison with existing experiments. However, as discussed near the end of this work, experimental realization of (5) may be possible.

IV. NATURE OF DEMIXING PHASE TRANSITION IN A POROUS MEDIUM

Do we expect that an Ising system confined to a porous medium generated as described in the previous section still experiences a phase transition? A related Ising system whose

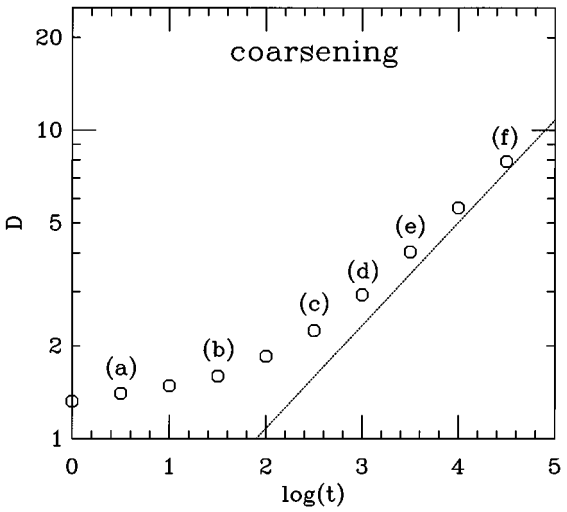

FIG. 2. Pore size D on a logarithmic scale as a function of $\log_{10}(t)$ where t is the growth time. The configurations that we used as the confining geometry in our simulation of the equilibrium properties of the confined Ising system are labeled (a)–(f). The dashed line is a curve with slope 1/3, and is added to show the asymptotic growth law of $D=(t/t_0)^{1/3}$, according to the Lifshitz-Slyozov-Wagner theory.

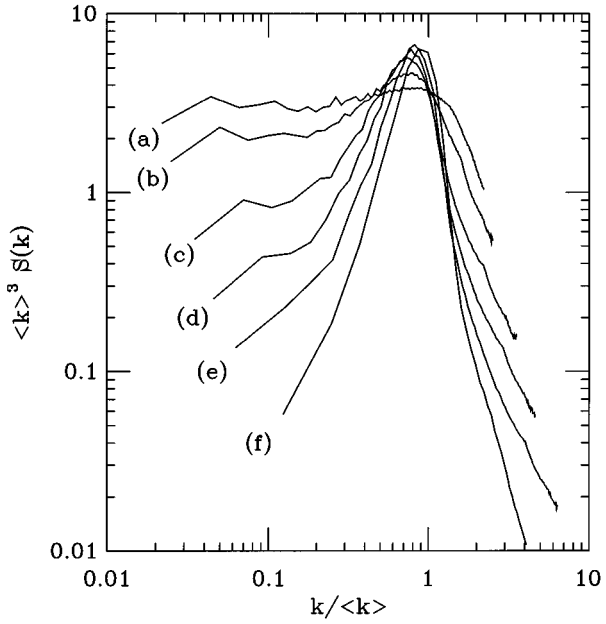

FIG. 3. Scaled density structure factor $\langle k\rangle^3 S(k)$ as a function of the scaled wave number $k/\langle k\rangle$ of samples with 128^3 sites, obtained by halting the phase-separation process after times (a)–(f).

critical behavior may be pertinent to our model is the randomly site-diluted Ising model. In the dilute Ising model only some randomly chosen fraction p of the lattice sites are occupied by spins: the remaining sites are empty. Below a critical occupancy fraction this model does not experience a phase transition; $p_c \approx 0.27$ to 0.31.[20] If no spinodal decomposition is carried out, our model corresponds to the dilute Ising model with an occupancy fraction of 50%, well above p_c, and it will have a phase transition. For larger pore sizes (increasing periods of spinodal decomposition) the connectivity of the spin-spin interactions is increased and thus we expect the phase transition to persist.

Given a sharp critical phase transition, the question of its universality class arises. The Harris criterion[21] tells us that the introduction of nonmagnetic weak quenched randomness (including constrained randomness[22]) into a system is expected to change the universality class when the specific-heat exponent α satisfies $\alpha>0$. Since $\alpha>0$ for the homogeneous Ising model in three dimensions, this indicates that the universality classes of the dilute Ising model and our model may each be different from that of the homogeneous Ising model.

TABLE I. Properties of porous media samples, obtained by halting the phase separation process at times (a)–(f). Second column: pore size D of these samples. Third column: critical temperature of the porous Ising model of the samples.

Porous medium configuration	D	$T_c(D)$
a	1.41	2.058 (12)
b	1.60	2.358 (12)
c	2.24	2.845 (12)
d	2.93	3.175 (12)
e	4.03	3.552 (12)
f	7.92	4.065 (12)

We are interested in whether our porous Ising model has the same critical phenomena as the dilute Ising model. Our porous medium is identical to a regular lattice in which those bonds are omitted that connect sites in the glass region to sites in the pores, in which case the influence of the glass

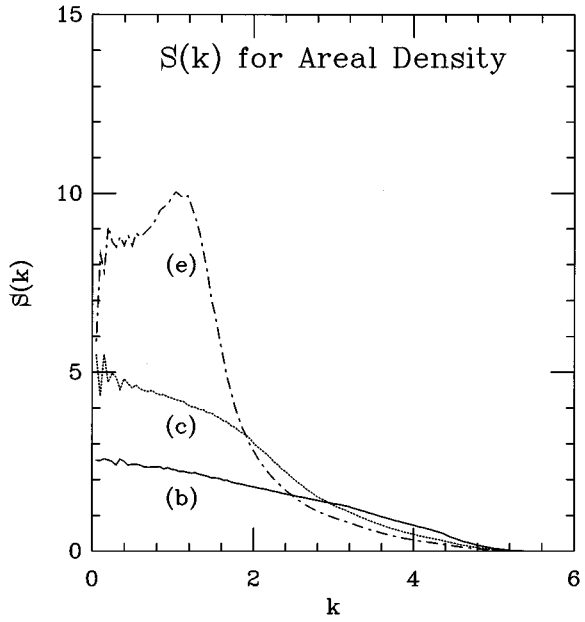

FIG. 4. Structure factor $S(k)$ for the surface density inside the porous medium, as a function of wave number k, for configurations (b), (c), and (e), obtained from configurations with 128^3 sites. To obtain these functions accurately, we averaged the structure factor over seven distinct configurations for each pore size. In contrast to the structure factor of the mass density, the structure factor of the areal density is flat at small wave vectors, indicating that in contrast to the spin density, the surface density is uncorrelated at long ranges.

region on our Ising model is felt through its surface. As the areal density (Fig. 4) of that surface does not show long-ranged correlations, and as it represents the density of absent bonds (and therefore the bond energy fluctuations), it would not be surprising if our porous Ising model has the same critical exponents as the dilute Ising model, although the topological structure of the pore region surely plays a role as well.

On the other hand, in contrast to the dilute Ising model in which the structure of the disorder is random ''white noise,'' the disorder in our system is correlated over long ranges: the structure factor of the lattice site density approaches zero with a power law for small k. Also, it has been suggested to us[23] that topological differences between our correlated pores and the random disorder in the dilute Ising model may make their critical behavior different. A direct way to decide this question is a large-scale computer simulation.

In addition to the critical exponents, we are also interested in the dependence of the critical temperature on the pore size. The ratio of the density of bonds in our porous Ising model to that of the pure Ising model is given by $1-c/D$, where c is some constant determined by the exact definition of D. Thus, the effective coupling in the confined Ising model may be viewed crudely as $1-c/D$ times that of the homogeneous system. Consequently, we might expect that the critical temperature is lower by the same factor:

$$T_c(D)/T_c(\infty)=1-c/D. \tag{6}$$

Another way of seeing this is to consider that the average coordination number in our system is diminished by a factor proportional to $1-c/D$ compared with the homogeneous system. The above dependence of T_c on the average pore size then follows from the linear mean-field dependence of the critical temperature on the coordination number.[24]

V. SIMULATING CRITICAL DEMIXING IN A POROUS MEDIUM

The appearance in our model of an extra length scale, the pore size D, that must be larger than the lattice spacing and small compared to the system size L, necessitates system sizes substantially larger than those that would be required for the simulation of a homogeneous Ising model. We considered porous medium configurations in which the pore size ranged from around 1.4 to 8.0 lattice spacings. A range of system sizes was required to do a finite-size scaling analysis. As the pore size should be substantially smaller than the system size, our system sizes ranged from $L=20$ to $L=128$.

Rather than single-spin Metropolis-type algorithms that are notoriously slow in random systems, we used a combination of two algorithms based on MC moves that flip many connected spins, called *clusters*. The first and primary algorithm is the parallel local cluster (PLC) algorithm,[15] which is based on the local-cluster algorithm.[25] In the PLC algorithm, the system is partitioned into some number N_{proc} of sublattices, the responsibility for each of which is assigned to one processor. The sequence of steps followed by each processor is as follows:

(1) Randomly pick a site s in the interior of the sublattice which is not in the ''glass'' region of the porous medium. This site is the first member of the cluster C under construction.

(2) Consider all neighboring sites of s, whose spins are aligned with the spin located at site s. With probability $1-\exp(-2J/k_BT)$ add each such neighbor to the cluster. Iteratively, apply the same procedure to all neighbor sites of sites newly added to C. If at any moment a site is added to C that is located on the border of the sublattice, cease the construction of C and restore the original spins to all sites in C.

(3) If the iteration in step 2 ends and no site located on the border of the sublattice is added to C, flip the spins located on all sites in C.

Steps 1–3 are repeated until on average each site has been included once in a cluster.

(4) Shift the lattice partition by some random vector, considering the periodic boundary conditions, and then repartition the system.

This procedure constitutes one PLC step. Subsequent steps are made by repeating the procedure from step 1. This procedure asymptotically samples the probability density $(1/Z)\exp(-H/k_bT)$, where the partition function Z normalizes the distribution. The complex system geometry imposed by the medium thus enters the algorithm only in that there are no Ising lattice sites in the glass region of the porous medium.

Although the PLC algorithm can be implemented very efficiently on a parallel computer,[15] because of its local nature it can take many steps to bring about a system-wide, true equilibration. The nonlocal Wolff algorithm does not experience this problem, and overcomes this weakness of the PLC algorithm, a slow equilibration over large distances, in only a few steps. Its drawback is however that it cannot be implemented efficiently on a parallel computer. We used a combination of both the PLC and the Wolff algorithms, and obtained a much more rapid equilibration than we would have experienced using either alone. The ratio of PLC steps to Wolff steps that we chose ranged from 1 to 10, depending on the system size. We based our choice on the equilibration and correlation times of the energy and magnetization.

Figure 5 shows a typical plot of the autocorrelation time for 64^3 and 128^3 realizations of our systems with the smallest pore size, as a function of reduced coupling K. The times are given in ''passes,'' each of which consists of one PLC step; sometimes (for the 64^3 system, once every five passes, for the 128^3 system, once every ten passes) a pass consists of a PLC step followed by a Wolff step. Typical runs consisted of 1000 total steps. Our runs started from configurations with random spin values assigned to the spin variables, and the results were found to agree with test runs which began with all spins up or all spins down. Typical ''wall clock'' times for each temperature run ranged from several minutes for a 1000 PLC/500 Wolff step 32^3 systems running on eight processors, to between 1 and 2 h per temperature for 1000 PLC/100 Wolff 128^3 systems running on 64 processors.

Both algorithms are less efficient in the ordered phase: the PLC algorithm generates clusters that are more likely to touch the sublattice boundaries and thus be rejected; the Wolff algorithm generates clusters that tend to become system spanning, resulting in much greater computer time requirements.

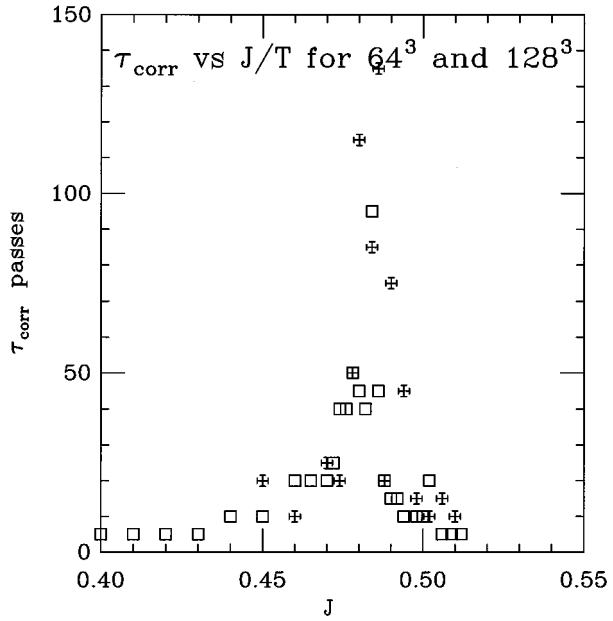

FIG. 5. Autocorrelation time $\tau_{\rm corr}$ as a function of the reduced coupling for 64^3 (squares) and 128^3 (plusses) realizations of the porous medium system with the smallest pore size.

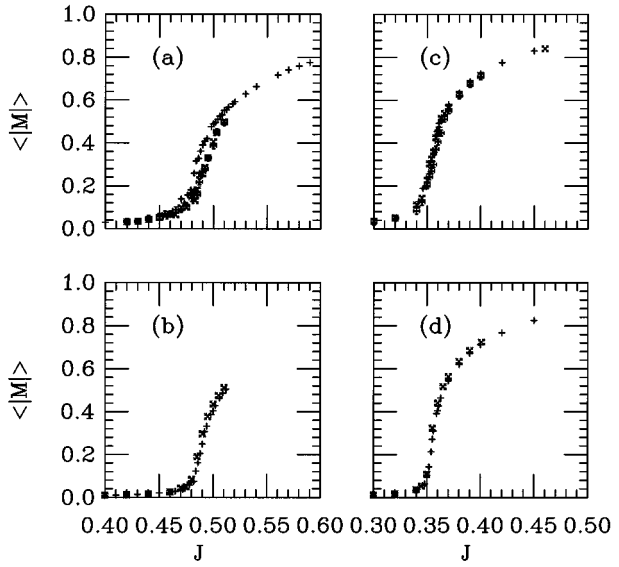

FIG. 6. Magnetization as a function of J for three different 32^3 realizations (upper plots) and three different 64^3 realizations (lower plots) of porous media with pore sizes $D=1.41$ (left plots) and $D=2.24$ (right plots). Some variation in T_c is evident for small pore sizes and small system sizes.

VI. CRITICAL TEMPERATURE AND EXPONENTS

A. Simulations and statistical methods

We generated porous medium configurations of sizes 20^3, 32^3, 64^3, 96^3, and 128^3. For each system size we generated six different realizations of the porous medium, with average pore size ranging from approximately $D=1.4$ to $D=8$ lattice constants, shown as the labeled points (a)–(f) in Fig. 2. As each realization is obtained by halting the growth process after some specified amount of time has elapsed and not when the configuration has a specified D, there is a small (1–3 %) variation in D between the different system sizes. For the smaller systems, the determination of D introduces statistical fluctuations that do not show any trend with system size. Therefore, rather than determining D directly from each configuration, we determine D from a 128^3 configuration that has run over exactly the same time interval.

For an Ising model confined to the pores of these configurations, we computed the average energy and the average magnitude of the magnetization (which corresponds to one half the binodal of the liquid system) as functions of temperature, as well as the specific heat and magnetic susceptibility obtained from the fluctuations in the former. The energy is

$$E=-J\left\langle \sum_{\langle ij\rangle} \sigma_i\sigma_j \right\rangle \tag{7}$$

and the magnetization is

$$M=\left\langle \left| \sum_i \sigma_i \right| \right\rangle, \tag{8}$$

where $\langle\rangle$ indicates a thermal average. The magnetic susceptibility χ and specific heat C are

$$T\chi=\langle M^2\rangle-\langle |M|\rangle^2 \tag{9}$$

and

$$T^2C=\langle E^2\rangle-\langle E\rangle^2. \tag{10}$$

In all these expressions we use dimensionless temperature $T\equiv 1/J$. Statistical errors in the magnetic susceptibility and specific heat were estimated using the ''bootstrap'' technique.[26]

In random lattice systems such as the random-field Ising model a considerable variation exists between the properties we study for different realizations of randomness. For this reason, we investigated the variation in E, M, χ, and C for different realizations of the porous medium with the same pore size. Figure 6(a) shows M for three different 32^3 porous medium configurations, for the smallest pore size class that we studied, (a). A small variation in the apparent T_c is evident. Figure 6(b), showing M for two distinct 64^3 realizations of the same pore size class, reveals that the differences from one realization to another are greatly diminished with increasing system size. Figures 6(c) and 6(d) show the same for a larger pore size class (c), indicating that the variations in M from one realization to the next are very small even for the 32^3 system. The variation for larger pore sizes than these is imperceptible from sample to sample.

The critical temperature and the exponents γ and ν may be extracted from the magnetic susceptibility using finite-size scaling. Near the critical temperature the Widom scaling hypothesis[27] tells us that the magnetic susceptibility of our system scales with system size as

$$\chi\sim L^{-\gamma/\nu}\tilde{\chi}(tL^{1/\nu}), \tag{11}$$

where $t=T/T_c-1$ and $\tilde{\chi}$ is a universal scaling function. Although neither the exponents nor T_c is known initially, the scaling relation can be used to determine these parameters by

plotting $\chi L^{\gamma/\nu}$ as a function of $tL^{1/\nu}$, and varying the parameters γ/ν, t, and $1/\nu$ until the multiple curves "collapse" onto one another.

From our value for ν we can determine the specific-heat exponent α indirectly, assuming the hyperscaling relation

$$d\nu = 2 - \alpha. \tag{12}$$

The scaling relation

$$\alpha + 2\beta + \gamma = 2 \tag{13}$$

allows for an indirect determination of the order-parameter exponent β.

Because of large statistical fluctuations in our specific-heat results, it was not possible to directly extract a numerical value for α. To obtain an independent determination of the order-parameter exponent β using our data for the magnetization, we followed the procedure of Binder[28] described by Hennecke.[29] Exactly at the critical temperature we expect the magnetization $M(T_c)$ of our systems to scale with system size according to

$$M_L(T_c) \sim L^{-\beta/\nu}, \tag{14}$$

where the prefactor is independent of L, though it might depend on the pore size. For systems of two sizes L_1 and L_2, we define

$$\xi_{L_1,L_2}(T) = \log_{L_1/L_2}\left(\frac{M_{L_1}(T)}{M_{L_2}(T)}\right). \tag{15}$$

The utility of this definition follows from $\xi_{L_1,L_2}(T_c) = -\beta/\nu$. When sets of curves $\xi_{L_1,L_2}(T)$ are plotted, for different choices of L_1 and L_2 for all the curves, the curves should all intersect in one point where $T = T_c$ and $\xi_{L_1,L_2}(T) = -\beta/\nu$.

B. Numerical results for the critical temperature and exponents

First we used finite-size scaling of the magnetic susceptibility according to Eq. (11). While plausible collapses can be achieved for fairly wide range of values for the exponents, the procedure is very sensitive to changes in the critical temperature and thus $T_c(D)$ may be accurately determined. Our results for $T_c(D)$ are tabulated in Table I, and plotted in Fig. 7, along with Eq. (6) for $c = 3.6$ [$T_c(\infty) \approx 4.512$ is the known critical temperature of the pure Ising model]. This line fits all the measurements to within better than 3%. Because the average site coordination number in our system is proportional to $1 - \text{const}/D$, the linear dependence of T_c on this quantity is consistent with the simple mean-field theory result mentioned in Sec. IV. The curve $T_c(D) = T_c(\infty) - cD^{(-1/\nu)}$ fits the data more poorly for $\nu < 1$, but cannot be ruled out completely.

Figure 8 shows our collapse data for all six pore sizes studied for $\gamma/\nu = 1.7$ and $1/\nu = 1.2$. We explored the ranges of γ/ν and $1/\nu$ that give a collapse of similar quality, resulting in $\gamma = 1.4 \pm 0.1$ and $\nu = 0.8 \pm 0.1$. There are correlations between the uncertainties in the two exponents, and a good collapse is not necessarily obtained for any choice of the pair γ and ν lying within the range. With this value for ν and the hyperscaling relation (12) we find $\alpha = -0.4 \pm 0.3$. Although it was not possible to extract a numerical value for α from finite-size scaling of the specific heat, we could conclude that α is negative, in agreement with the indirectly determined value for α. This is what is expected in light of the Harris criterion. An indirect determination of β with scaling relation (13) gives $\beta = 0.5 \pm 0.1$.

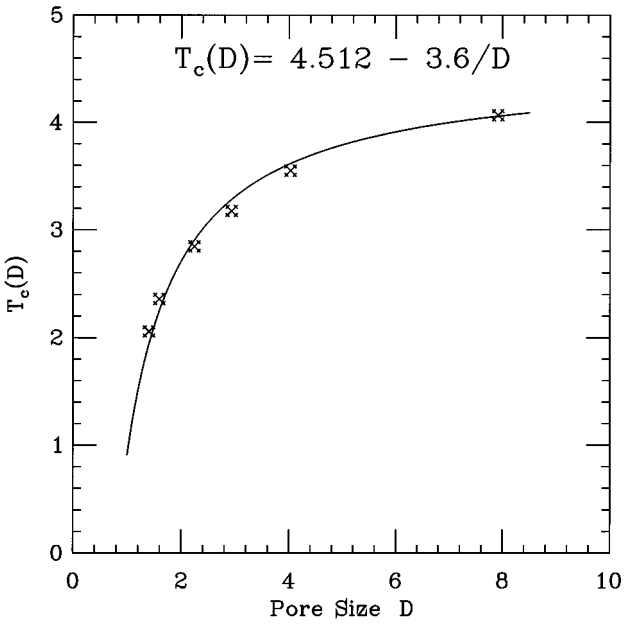

FIG. 7. Critical temperature as a function of typical pore radius, obtained by finite-size scaling. The line is given by $T_c(D) = T_c(\infty) - c/D$, in which $T_c(\infty) = 4.512$ and $c = 3.6$.

Figure 8 shows that the same exponents bring about a collapse of the susceptibility data for all pore sizes D; this

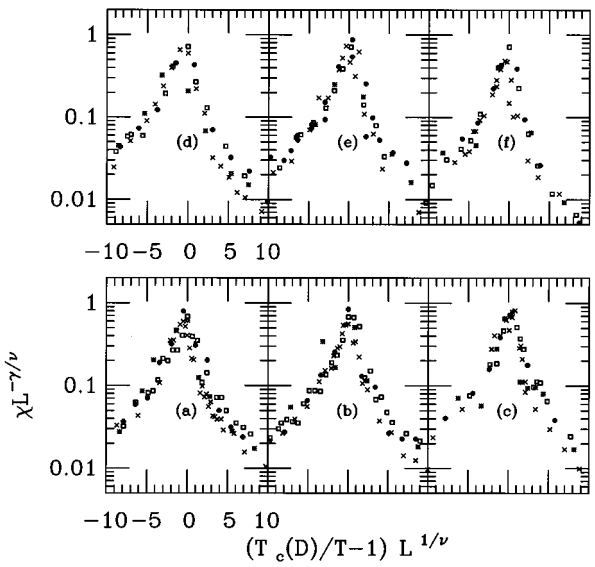

FIG. 8. Collapse of all our data points for the magnetic susceptibility, by plotting $\chi L^{-\gamma/\nu}$ as a function of $[T_c(D)/T - 1]L^{1/\nu}$, with $\gamma/\nu = 1.7$ and $1/\nu = 1.2$, and the critical temperature $T_c(D)$ as given in Table I. Note that $[T_c(D)/T - 1] = (1 - T/T_c) + O[(1 - T/T_c)^2]$. System sizes are 32^3 (crosses), 64^3 (squares), 96^3 (plusses), and 128^3 sites (bursts). The labels in the figures denote the pore sizes (see Table I).

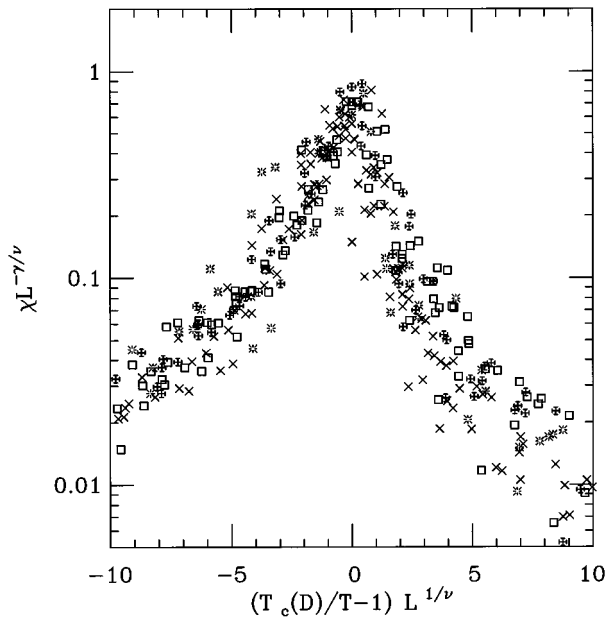

FIG. 9. Data of Fig. 8, combined in a single plot to show the common scaling function for all pore sizes.

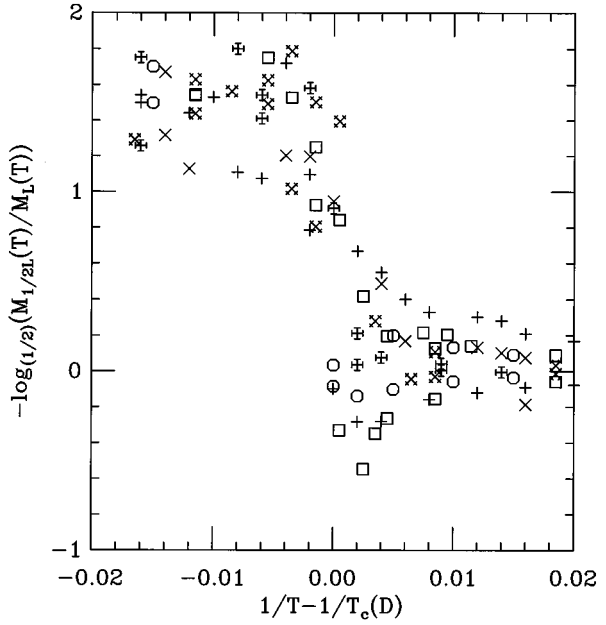

FIG. 10. The function $\xi_{32,64}(T)$ and $\xi_{64,128}(T)$, defined in the text, as a function of $1/T-1/T_c(D)$ for all of our pore size data. The curves have a common intersection point corresponding to $\beta/\nu=0.79\pm0.06$.

indicates that systems with all pore sizes are in the same universality class. Could the universal scaling function itself be the same for all pore sizes? If so, a more general form of the scaling relation (11) might hold near $T_c(D)$:

$$T\chi(T)\sim L^{\gamma/\nu}\tilde{\chi}(tL^{1/\nu}), \tag{16}$$

where now $t=T/T_c(D)-1$ takes into consideration the pore size dependence of the critical temperature, and the scaling form is otherwise independent of D. Figure 9 shows such a collapse. The data of Fig. 8 have been combined into a single plot, showing that near $T_c(D)$, the curves all appear to collapse onto one common curve, so that with the exception of the dependence of T_c on pore size, the critical behavior of all these systems is the same. This again indicates that there is one universality class, independent of pore size. The absence of additional prefactors of the scaling function that depend on the pore size is unexpected.

The exponent β can be obtained directly from a collapse of the magnetization curves, as outlined in the previous section. We discovered that the prefactor in Eq. (14), like that for the susceptibility, is apparently independent of the pore size D, so that when the sets of curves $\xi_{L_1,L_2}[T-T_c(D)]$ are plotted together for different D, the resulting curves have a common intersection point. The results are shown plotted in Fig. 10 for $(L_1,L_2)=(32,64)$ and $(64,128)$. For both system sizes L_1 and L_2 the simulation must be carried out at the same temperatures in order for ξ to be computed; therefore it was not possible for us to use all of our simulation data for these curves. From the common intersection point of these curves, we obtain a value $\beta/\nu=0.79\pm0.06$. Using our determination of ν, we obtain $\beta=0.65\pm0.13$. Considering the uncertainties in this value for β and in our previous derived value, the two are in agreement.

All the exponents discussed in this section are summarized in the first column of Table II. In the second column of this table, we give the exponents for the pure Ising model, as reported by Ferrenberg and Landau.[30] It is clear that the porous and pure Ising models have different exponents, and therefore are in different universality classes.

Our exponents are similar to those found in simulations of the dilute Ising model. Overall, there is a disparity in the exponents reported for that model between results obtained using field-theoretic techniques[31,32] and between those of simulation and experiment.[33–35,29] Field-theoretic values[32,31] for the exponent γ are larger than that for the pure Ising model ($\gamma_{\text{Bulk}}=1.239\pm0.001$), ranging from 1.321 to 1.335. Simulation results and experimental values suggest an exponent that is even larger, with reported values varying from 1.3 to 1.5.[33] Some authors have reported a dependence of γ on the dilution fraction that saturates for strong dilution to 1.5.[36] In this work, in our system we find $\gamma=1.4\pm0.1$.

The field-theoretic values for the exponent β are again slightly larger than those reported for the pure system ($\beta_{\text{Bulk}}=0.326\pm0.004$), typically around 0.348.[32,31] Simulation results are again substantially higher, with Hennecke[29] reporting a value obtained by Monte Carlo simulation of 0.42 ± 0.04 for a dilution fraction of 40%. The indirect and direct determinations of β for our system are $\beta=0.5\pm0.1$ and $\beta=0.65\pm0.13$, respectively. The exponents ν from field-theoretic treatments of the dilute Ising model are close to 0.68, again larger than the pure Ising value of

TABLE II. Exponents extracted from our simulations, together with those reported for the pure 3D Ising system.

Exponent	This work	Bulk Ising
ν	0.81 ± 0.1	0.627 ± 0.002
γ	1.4 ± 0.1	1.239 ± 0.003
β	0.65 ± 0.13	0.326 ± 0.004

0.627 ± 0.002, though substantially below the value of 0.78 ± 0.01 (Ref. 29) reported from simulation. In our model we find $\nu = 0.81 \pm 0.1$.

We are not aware of any determinations of the exponent α for the dilute Ising model by simulation, though field-theoretic calculations of -0.013 (Ref. 32) and -0.034 (Ref. 31) have been reported, which is consistent with the observation in our system that α is negative. On the basis of comparison the sets of critical exponents for the porous Ising model and the dilute Ising model, we propose that they are in the same universality classes.

VII. EFFECT OF VARIATIONS IN PORE STRUCTURES

We also calculated the magnetization and magnetic susceptibility of configurations with fundamentally different pore structures. We first wanted to understand what would happen if there were some large voids inside a porous medium in addition to the more regular pore pattern, a situation that might arise experimentally. This was investigated by taking a 64^3 Vycor-like sample for which the coarsening process was halted at time (c) so that it had a typical pore radius $D_1 = 2.24$. Then a 32^3 hole was cut, leaving one large pore with size $D_2 \approx 32$, surrounded by smaller pores.

The resulting magnetic susceptibility, plotted in Fig. 11(a), shows two distinct peaks, one located close to the critical temperature of the pure Ising model, and the other located close to the critical temperature of the Vycor-like sample before the hole was cut into it. The corresponding binodal is included in an inset in Fig. 11(a) and shows a small protrusion on top of the original binodal for the porous sample. The appearance of a second peak in the magnetic susceptibility located around the critical temperature of the pure Ising model is not surprising, since as long as the correlation length is smaller than $0.5D_2$, the radius of the big pore, the spins located in the interior of the big pore will behave identically to ones in the homogeneous Ising model. It is thus not surprising, that if in experiments critical exponents would be obtained from measurements in this region of the protrusion, they would be in the universality class of the pure Ising model.

We further increased the system size by duplicating the system in each direction to obtain a 128^3 system with eight large 32^3 holes. The binodal for this larger system is shown in Fig. 11(b). As the first peak (located at the critical temperature of the pure Ising model) does not become sharper with increasing system size (in contrast to the second larger peak at larger J), we conclude that this peak does not correspond to a phase transition. This indicates that until the true phase transition at $J \approx 0.38$ the large pores cannot communicate and fluctuate independently.

If two distinct peaks in the magnetic susceptibility arise when two distinct pore radii are present in the system, might it be that what we assumed to be one peak in the magnetic susceptibility in our porous media actually is the sum of a spectrum of peaks, corresponding to a spectrum of pore radii? We generated a second type of structure with two distinct pore sizes by combining two model media with pore sizes D_1 and D_2. We did this by performing a logical OR operation on the pore regions to obtain a porous medium

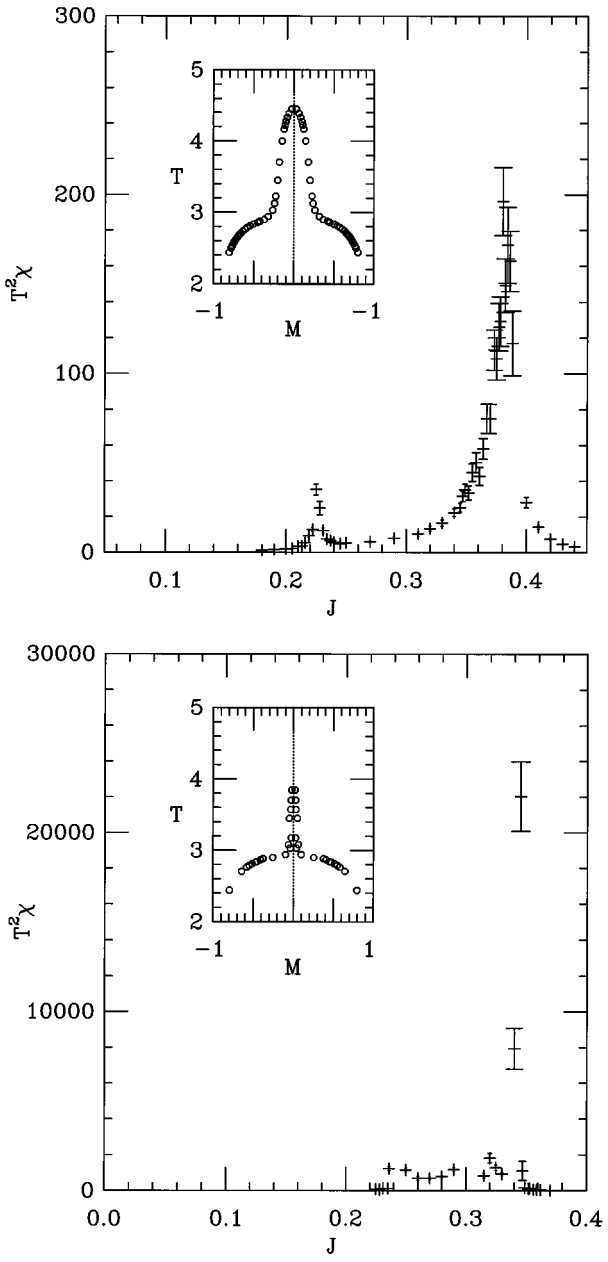

FIG. 11. (Top) Magnetic susceptibility of the Ising model confined to a porous medium in which a big hole is excavated. The porous medium is generated by coarsening a 64^3 system over $t = 1000$ time steps, corresponding to configurations (c), with typical pore size $D = 2.24$, in which one big pore is excavated of size 32^3. The inset shows the binodal. (Bottom) The magnetic susceptibility is plotted for the same system, but duplicated in each direction, resulting in a 128^3 system with eight pores of 32^3 sites. Again, the inset shows the binodal.

with a porosity around 75%. This system has only one peak in its magnetic susceptibility; this peak occurs at a temperature different from the T_c for the two media that were combined. This is a strong indication that a spread in pore sizes, inevitably present in our configurations, does not cause a ''blurred'' combination of phase transitions, but that the Ising model confined to a porous medium has one clear phase transition.

VIII. LINK WITH EXPERIMENTS

In experiments to date studying demixing in Vycor, the glass had a preference for one phase over the other. Our model has no such preference, although this could be accounted for simply by adding pore surface fields, and our algorithm could be modified to study this situation (a slight shift in overall chemical potential, i.e., a weak magnetic field throughout the system, should also be included in the resulting asymmetric model). The statistics of such surface fields (like the ''broken bonds'' of this paper) will be determined by the surface area density fluctuations. Thus, we expect the structure factor of such surface magnetic fields to be uncorrelated at long distances. This feature is essential to the arguments of Brochard and de Gennes[8] which suggest that liquid-vapor critical phenomena inside a Vycor-like medium will be that of the random-field Ising model. Surface fields are thereforce expected to further change the static critical phenomena. However, we also expect drastic slowing down of numerical simulations which is the reason why we did not include surface fields in this study.

It might be possible to chemically treat Vycor such that it has an equal surface interaction with each component of a binary mixture, and thereby find an experimental realization of the porous Ising model studied in this paper. Methods to do this have been developed by Durian and Franck[37] in studies of wetting phenomena on borosilicate glass substrates. They performed capillary rise experiments of carbon disulfate-nitromethane mixtures, dosing the borosilicate glass with hexamethyldisilizane in order to reduce the attraction of nitromethane. Another material that might be used instead of Vycor is porous gold. Samples of porous gold have been produced with a pore size ranging over about two decades.[38] Wetting properties of gold surfaces have been successfully manipulated by Abbott *et al.*[39]

IX. CONCLUSIONS

The experimental evidence for whether phase separation[1,2] and two-phase coexistence[40] of liquids confined to porous media have the same critical exponents as unconfined liquid systems has been so far inconclusive. In this work, we have considered a simple model that incorporates only the geometric effects of a porous medium such as Vycor, and we find that the effect of confinement alone gives rise to a different universality class for these transitions. Our results indicate that one should expect different critical exponents in these systems, in comparison with their unconfined counterparts.

The exponents of the porous Ising model coincide with those estimated for the dilute Ising model, and so we conclude that they are in the same universality classes. The large uncertainties in our exponents and the disparity between theoretical and computational results for that system make this conclusion provisional. The uncorrelated long-distance fluctuations of pore surface area density (which we observe) provides a rationale to link these two models.

An addition to our model, which we believe would make it describe experimental situations that have already been studied, is a uniform field acting at the pore surface. This would account for symmetry-breaking surface interactions of the glass with the two components of a binary mixture, or with the two phases of a liquid-vapor system, which will generally occur for real porous media. We anticipate that this addition will yield random-field Ising behavior.

ACKNOWLEDGMENTS

Geoffrey Chester, Karen Dahmen, Eugene Kolomeiskii, Mark Newman, Jim Sethna, and Ben Widom are gratefully acknowledged for their help in this research. The work of T.M.F. was financially supported by the Department of Education. The work of G.T.B. was supported by the National Science Foundation under Contracts No. ASC-93-10244 and No. DMR-91-21654 through the MRL program, the Materials Science Center, and the Cornell National Supercomputer Facility. J.M. was supported by a grant from the Meyer Foundation. This research was conducted using the resources of the Cornell Theory Center, which receives major funding from the National Science Foundation, and New York State. Additional funding comes from the Advanced Research Projects Agency, the National Institutes of Health, IBM Corporation and other members of the Center's Corporate Research Institute.

---

*Current address: Rechenzentrum, Max-Planck-Institut für Plasmaphysik Boltzmannstrasse 2, D-85748 Garching bei München.

†Current address: Institute for Advanced Study, Princeton, NJ 08540.

[1] A.P.Y. Wong and M.H.W. Chan, Phys. Rev. Lett. **65**, 20 (1990); **65**, 2567 (1990).

[2] A.P.Y. Wong, S.B. Kim, W.I. Goldburg, and M.H.W. Chan, Phys. Rev. Lett. **70**, 954 (1993).

[3] S.B. Dierker and P. Wiltzius, Phys. Rev. Lett. **58**, 1865 (1987).

[4] M.C. Goh, W.I. Goldburg, and C.M. Knobler, Phys. Rev. Lett. **58**, 1008 (1987).

[5] P. Wiltzius, S.B. Dierker, and B.S. Dennis, Phys. Rev. Lett. **62**, 804 (1989).

[6] S.B. Kim, J. Ma, and M.H.W. Chan, Phys. Rev. Lett. **71**, 2268 (1993).

[7] D. Finotello, K.A. Gillis, A. Wong, and M.H.W. Chan, Phys. Rev. Lett. **61**, 1954 (1988).

[8] F. Brochard and P-G. de Gennes, J. Phys. (Paris) Lett. **44**, 785 (1983); P-G. de Gennes, J. Phys. Chem. **88**, 6469 (1984).

[9] A.N. Berker, J. Appl. Phys. **70**, 5941 (1991); Physica (Amsterdam) **194A**, 72 (1993); A. Maritan, M. Cieplak, M.R. Swift, F. Toigo, and J.R. Banavar, Phys. Rev. Lett. **69**, 221 (1992).

[10] A. Falicov and A.N. Berker, Phys. Rev. Lett. **74**, 426 (1995).

[11] K. Uzelac, A. Hasmy, and R. Jullien, Phys. Rev. Lett. **74**, 422 (1995).

[12] P. Levitz, G. Ehret, S. K. Sinha, and J. M. Drake, J. Chem. Phys. **95**, 6151 (1991).

[13] A.J. Bray, Adv. Phys. **43**, 357 (1994).

[14] G.T. Barkema, J.F. Marko, and J. de Boer, Europhys. Lett. **26**, 653 (1994); J.F. Marko and G.T. Barkema, Phys. Rev. E **52**, 2522 (1995).

[15] G.T. Barkema and T. MacFarland, Phys. Rev. E **50**, 1623 (1994).

[16] U. Wolff, Phys. Rev. Lett. **62**, 361 (1989).

[17] C. Yeung, Phys. Rev. Lett. **61**, 1135 (1988).

[18] I.M. Lifshitz and V.V. Slyozov, J. Phys. Chem. Solids **19**, 35 (1961); C. Wagner, Z. Elektrochem. **65**, 581 (1961).

[19] A. Shinazaki and Y. Oono, Phys. Rev. Lett. **66**, 173 (1991).
[20] A. Bobak, M. Jascur, and S. Mockoviak, Phys. Status Solidi B **183**, 565 (1994).
[21] A.B. Harris, J. Phys. C **7**, 1671 (1974).
[22] A. Weinrib and B.I. Halperin, Phys. Rev. B **27**, 413 (1983).
[23] E. B. Kolomeisky (private communication).
[24] F. Reif, in *Fundamentals of Statistical and Thermal Physics* (McGraw-Hill, New York, 1965).
[25] G.T. Barkema and J.F. Marko, Phys. Rev. Lett. **71**, 2070 (1993).
[26] B. Efron and R. Tilshirani, Stat. Sci. **1**, 54 (1986).
[27] B. Widom, J. Chem. Phys. **43**, 3892 (1965).
[28] K. Binder, Z. Phys. B **43**, 119 (1981).
[29] M. Hennecke, Phys. Rev. B **48**, 6271 (1993).
[30] A.M. Ferrenberg and D.P. Landau, Phys. Rev. B **44**, 5081 (1991).
[31] G. Jug, Phys. Rev. B **27**, 609 (1983).
[32] I.O. Mayer, J. Phys. A **22**, 2815 (1989).
[33] J.S. Wang, M. Woehlert, H. Muhlenbein, and D. Chowdhury, Physica A **166**, 173 (1990).
[34] J.S. Wang and D. Chowdhury, J. Phys. (Paris) **50**, 2905 (1989).
[35] K.E. Newman and E.K. Riedel, Phys. Rev. B **25**, 264 (1982).
[36] H.-O. Heuer, Europhys. Lett. **12**, 551 (1990).
[37] D.J. Durian and C. Franck, Phys. Rev. Lett. **59**, 555 (1987).
[38] R. Li and K. Sieradzki, Phys. Rev. Lett. **68**, 1165 (1992).
[39] N.L. Abbott, J.P. Folkers, and G.M. Whitesides, Science **257**, 1380 (1992).
[40] J. Ma, S.B. Kim, L.W. Hrubesh, and M.H.W. Chan, J. Low Temp. Phys. **93**, 945 (1993).